IOPscience iopscience.iop.org

Home Search Collections Journals About Contact us My IOPscience

Dark breathers in Klein-Gordon lattices. Band analysis of their stability properties

This content has been downloaded from IOPscience. Please scroll down to see the full text.

2002 New J. Phys. 4 72

(http://iopscience.iop.org/1367-2630/4/1/372)

View the table of contents for this issue, or go to the journal homepage for more

Download details:

IP Address: 150.214.230.47
This content was downloaded on 13/04/2015 at 13:21

Please note that terms and conditions apply.

New Journal of Physics
An Institute of Physics and Deutsche Physikalische Gesellschaft Journal

Dark breathers in Klein–Gordon lattices. Band analysis of their stability properties

A Alvarez[1], **J F R Archilla**[2], **J Cuevas**[2] **and F R Romero**[1]

[1] Group of Nonlinear Physics of the University of Sevilla, Facultad de Física, P 5, Avda. Reina Mercedes s/n, 41012 Sevilla, Spain

[2] Group of Nonlinear Physics of the University of Sevilla, Dep. Física Aplicada I en ETSI Informática, Avda. Reina Mercedes s/n, 41012 Sevilla, Spain

E-mail: azucena@us.es (A Alvarez)

New Journal of Physics **4** (2002) 72.1–72.19 (http://www.njp.org/)
Received 1 August 2002
Published 8 October 2002

Abstract. Discrete bright breathers are well known phenomena. They are localized excitations that consist of a few excited oscillators in a lattice and the rest of them having very small amplitude or none. In this paper we are interested in the opposite kind of localization, or discrete dark breathers, where most of the oscillators are excited and one or a few units of them have very small amplitude. We investigate, using band analysis, Klein–Gordon lattices at frequencies not close to the linear ones. Dark breathers at low coupling are shown to be stable for Klein–Gordon chains with soft on-site potentials and repulsive dispersive interaction, and with hard on-site potentials and attractive dispersive interactions. At higher coupling dark breathers lose their stability via subharmonic, harmonic or oscillatory bifurcations, depending on the model. However, most of these bifurcations are harmless in the sense that they preserve dark localization. None of these bifurcations disappear when the system is infinite. Dark breathers in dissipative systems are found to be stable for both kinds of dispersive interaction.

1. Introduction

It is well known that intrinsic localized modes (also called *discrete breathers*) are exact, periodic and localized solutions that can be obtained in a large variety of nonlinear discrete systems. They are becoming a new paradigm for understanding many aspects of the behaviour of discrete systems (for a review, see, e.g., [1, 2]). Mackay and Aubry [3] proved analytically their existence and the conditions for their stability [1], under rather general hypotheses. Since then, many accurate numerical methods have been used to obtain breathers as exact numerical solutions up to machine precision [4], which permits the analysis of breather properties. Thus, for a given

 © IOP Publishing Ltd and Deutsche Physikalische Gesellschaft

model, it is possible to perform a numerical study of the ranges of existence and stability in the parameter space.

The term discrete breather is usually understood as a localized, periodic solution in a discrete system, but with a small number of excited oscillators. When only one oscillator has large amplitude it is known as a *one-site breather*. When more than one oscillator has large amplitude, the term *multibreather* is used. Hereafter, we will use the term *bright breather* when there are one or a few oscillators vibrating with large amplitude whereas the rest of them oscillate with small amplitude.

However, localization can be manifested in a different way, which consists of all the oscillators vibrating with large amplitude except one or a few of them oscillating with very small amplitude. The natural name for these entities is *dark breathers*, analogously to the well known term *dark solitons*. For the nonlinear Schrödinger equations, which govern both nonlinear optical modes in fibres and dilute Bose–Einstein condensates, two different kinds of scalar soliton solution, *bright and dark*, are known [5, 6]. Thus, a dark soliton is a solution which has a point with zero amplitude, that is, a soliton defining the absence of matter or energy. Since then, many papers have appeared referring to theoretical and experimental results relating to these entities. The effects of discreteness on the properties and propagation dynamics of dark solitons have been analysed in the discrete nonlinear Schrödinger (DNLS) equation, which is thought to be a good approximation for frequencies close to the linear frequency [7]–[11], the last one also with numerics on actual Klein–Gordon systems. It is worth remarking that some examples of dark localization have been observed experimentally [12], and some structural properties have been analysed in [13].

In this paper, we perform an analysis of the existence and stability of dark breathers for different models based on the properties of the band structure of the Newton operator. We have found that there exist stable dark breathers for a variety of one-dimensional Klein–Gordon lattices. For soft on-site potentials, dark breathers are stable only for repulsive dispersive interaction and for hard on-site potentials the stability found is for attractive interaction. These results agree with the ones that have been found for the DNLS approximation in [14] as a consequence of the modulational instability of the constant amplitude background.

It is not clear in which physical systems dark breathers can play a significant role. A possibility is DNA; we conjecture that dark breathers can occur in DNA chains at high temperature, close to thermal denaturation [15]. In this situation, a great number of molecules are vibrating with high amplitude, whereas a few of them could be almost at rest.

This paper is organized as follows: in section 2, we describe the proposed Klein–Gordon models and the resulting evolution equations. In section 3, we expose the tools for calculating dark breathers, and we explicitly show that the theorem of existence of Mackay and Aubry gives an affirmative answer to the question of existence of dark breathers. In section 4, we expose the method for the analysis of the linear stability of breather solutions using both the Floquet multipliers and Aubry band theory. In section 5, we investigate the stability of dark breathers for chains with soft on-site potential and attractive interactions between the particles. We show that it is not possible to obtain stable dark breathers for every value of the coupling parameter. This negative result suggested us to consider the study of chains with repulsive interactions between particles. Our results confirm that in this case there exist stable dark breathers up to significant values of the coupling. In section 6, lattices with hard on-site potentials are considered. For these cases, dark breathers are stable provided that particles interact through an attractive potential. Dark breathers become unstable through subharmonic, harmonic and oscillatory bifurcations

depending on the type of on-site potential. In section 7, we show that neither subharmonic nor oscillatory bifurcations disappear in infinite systems. Section 8 shows that dark breathers in dissipative systems are stable. The paper concludes with a short summary of the main results and some prospects in section 9.

2. Models

We study one-dimensional, anharmonic, Hamiltonian lattices of the Klein–Gordon type. The Hamiltonian is given by

$$H = \sum_n (\tfrac{1}{2}\dot{u}_n^2 + V(u_n)) + \varepsilon W(u) \tag{1}$$

where u_n are the coordinates of the oscillators referred to their equilibrium positions; $V(u_n)$ represents the on-site potential; u represents the set of variables $\{u_n\}$ and $\varepsilon W(u)$ represents the coupling potential, with ε being a parameter that describes the strength of the coupling. We suppose initially that ε is positive and $W(u)$ is given by

$$W(u) = \tfrac{1}{2}\sum_n (u_{n+1} - u_n)^2. \tag{2}$$

This interaction is attractive because a nonzero value of a variable tends to increase the values of the neighbouring variables with the same sign. The on-site potential is given by

$$V(u_n) = \tfrac{1}{2}\omega_0^2 u_n^2 + \phi(u_n) \tag{3}$$

with $\phi(u_n)$ being the anharmonic part of the potential. The variables are scaled so that all the particles in the lattice have mass unity and the linear frequency $\omega_0 = 1$. The dynamical equations for this system are

$$\ddot{u}_n + \omega_0^2 u_n + \phi'(u_n) + \varepsilon(2u_n - u_{n-1} - u_{n+1}) = 0. \tag{4}$$

These equations do not have analytical solutions and must be solved numerically. The solutions depend obviously on the chosen potentials $V(u_n)$ and $W(u)$. We will analyse the system for several $V(u_n)$ and coupling interactions $W(u)$. These models appear in many physical systems; a known example, with a suitable on-site potential $V(u_n)$, is the Peyrard–Bishop model for DNA [15], where the variables u_n represent the stretching of the base pairs.

3. Dark breather existence

We look for spatially localized, time-reversible and time-periodic solutions of equations (4) with a given frequency ω_b and a continuous second derivative. Therefore, the functions $u_n(t)$ can be obtained up to machine precision by truncated Fourier series of the form

$$u_n(t) = z_0 + \sum_{k=1}^{k=k_m} 2z_n^k \cos(k\omega_b t). \tag{5}$$

We distinguish three types of solution of the isolated oscillators that can be coded in the following way: $\sigma_n = 0$ for an oscillator at rest ($u_n(t) = 0, \forall t$); $\sigma_n = +1$ for an excited oscillator with frequency ω_b and $u_n(0) > 0$; finally, $\sigma_n = -1$ for an excited oscillator with frequency ω_b and $u_n(0) < 0$. Time-reversible solutions of the whole system at $\varepsilon = 0$ (anticontinuous limit) can be referred to by a coding sequence $\sigma = \{\sigma_n\}$. Therefore, $\sigma = \{0, \ldots, 0, 1, 0, \ldots, 0\}$ corresponds

to a one-site breather. Other codes can be $\sigma = \{0, \ldots, 0, 1, 1, 0, \ldots, 0\}$ for a symmetric two-site breather, and $\sigma = \{1, \ldots, 1, 0, 1, \ldots, 1\}$ for a one-site dark breather (this case correspond to the background in phase).

The method for calculating dark breathers is based on the general methods for obtaining breathers [4, 16]–[19].

The existence theorem by MacKay and Aubry [3] establishes that every solution at the anticontinuous limit corresponding to a code sequence can be continued up to a certain value of the coupling parameter $\varepsilon_c \neq 0$, as long as the following two hypotheses are fulfilled.

- The orbits of the uncoupled excited oscillators with the chosen frequency have to be such that $\frac{\partial \omega_b}{\partial I} \neq 0$, where $I = \int p \, \mathrm{d}q$ is the action variable of the oscillator. That is, the oscillator is truly nonlinear at that frequency.
- The frequency of the orbit must be such that $p\omega_b \neq \omega_0$ for any integer p. That is, none of the breather harmonics coincide with the linear frequency ω_0.

Therefore, this theorem gives an immediate answer to the question of the existence of dark breathers as they are obtained by continuation of the configuration mentioned above $\sigma = \{1, \ldots, 1, 0, 1, \ldots, 1\}$. However, the theorem does not give an estimate for the value of the coupling ε_c where the dark breather ceases to exist. Dark breathers have to be calculated numerically for each value of the coupling parameter, also it is worth investigating whether dark breathers are stable or not, and if they are stable, up to which value of the coupling parameter.

4. Dark breather stability

The stability analysis of a given breather solution can be performed numerically [1, 19]–[21]. The linearized equations corresponding to perturbations of this solution are

$$\ddot{\xi}_n + \omega_0^2 \xi_n + \phi''(u_n)\xi_n + \varepsilon(2\xi_n - \xi_{n-1} - \xi_{n+1}) = 0 \tag{6}$$

where $\xi = \{\xi_n(t)\}$ represents a small perturbation of the solution of the dynamical equations, $u(t) = \{u_n(t)\}$. The linear stability of these solutions can be studied by finding the eigenvalues of the Floquet matrix $\mathcal{F}_0$, called Floquet multipliers. The Floquet matrix transforms the column matrix with elements given by $\xi_n(0)$ and $\pi(0) \equiv \dot{\xi}_n(0)$ into the corresponding column matrix with elements $\xi_n(T_b)$ and $\pi(T_b) \equiv \dot{\xi}_n(T_b)$ for $n = 1, \ldots, m$ and $T_b = 2\pi/\omega_b$, that is

$$\begin{pmatrix} \{\xi_n(T_b)\} \\ \{\pi_n(T_b)\} \end{pmatrix} = \mathcal{F}_0 \begin{pmatrix} \{\xi_n(0)\} \\ \{\pi_n(0)\} \end{pmatrix}. \tag{7}$$

The Floquet matrix $\mathcal{F}_0$ can be obtained, choosing zero initial conditions except for one position or momentum equal to unity, and integrating numerically equation (6), a time span of a breather period. The final positions and momenta give the elements of the corresponding column of the Floquet matrix. In order to get accurate results [22], we have used a symplectic integrator. Equation (6) can be written as an eigenvalue equation

$$(\mathcal{N}(u(t), \varepsilon) \cdot \xi)_n = E\xi_n \tag{8}$$

where $\mathcal{N}(u(t), \varepsilon)$ is called the Newton operator. The solutions of equation (6) can be described as the eigenfunctions of $\mathcal{N}$ for $E = 0$. The fact that the linearized system is Hamiltonian and real implies that the Floquet operator is a real and symplectic operator. The consequence is that if λ is an eigenvalue, then $1/\lambda$, λ^* and $1/\lambda^*$ are also eigenvalues, and therefore a necessary condition for linear stability is that every eigenvalue has modulus one, that is, they are located at the unit

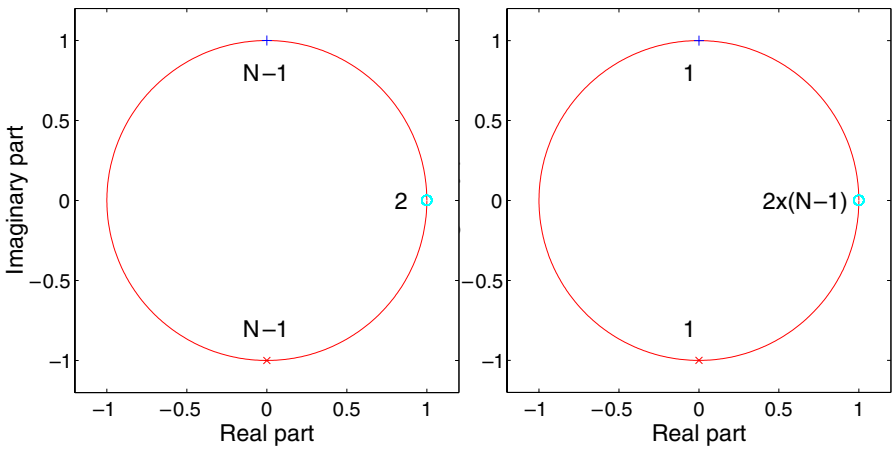

Figure 1. Floquet multipliers at zero coupling for (left) a bright breather and (right) a dark breather with the numbers of identical multipliers.

circle in the complex plane. Besides, there is always a double eigenvalue at $1 + 0i$ from the fact that the derivative $\{\dot{u}_n(t)\}$ is always a solution of (8) with $E = 0$.

The Floquet multipliers at the anticontinuous limit $(\varepsilon = 0)$ can be easily obtained for bright and dark breathers. If an oscillator at rest is considered, equation (6) becomes

$$\ddot{\xi}_n + \omega_0^2 \xi_n = 0 \tag{9}$$

with solution $\xi(t) = \xi_0 \mathrm{e}^{\mathrm{i}\omega_0 t}$, and therefore, the corresponding eigenvalue of $\mathcal{F}_0$ is $\lambda = \exp(\mathrm{i}2\pi\omega_0/\omega_b)$. If an oscillator is excited, equation (6) becomes

$$\ddot{\xi}_n + \omega_0^2 \xi_n + \phi''(u_n)\xi_n = 0. \tag{10}$$

This equation has $\dot{u}_n(t)$ as a solution, which is periodic and therefore with Floquet multiplier $\lambda = 1$. Thus, for a bright breather, we have, taking into account their multiplicity, $2(N-1)$ eigenvalues corresponding to the rest oscillators at $\exp(\pm\mathrm{i}2\pi\omega_0/\omega_b)$ and two at $+1$ corresponding to the excited one. For a dark breather at the anticontinuous limit there are $2(N-1)$ eigenvalues at $+1$, and a couple of conjugate eigenvalues at $\exp(\pm\mathrm{i}2\pi\omega_0/\omega_b)$.

Figure 1 shows the Floquet multipliers for both a bright and a dark breather at the anti-continuous limit $\varepsilon = 0$. When the coupling ε is switched on, these eigenvalues move on the complex plane as continuous functions of ε, and an instability can be produced only in three different ways [1]:

(a) a couple of conjugate eigenvalues reaches the value $1 + 0\mathrm{i}$ $(\theta = 0)$ and leaves the unit circle along the real line (harmonic bifurcation);

(b) a couple of conjugate eigenvalues reaches -1 $(\theta = \pm\pi)$ and leaves the unit circle along the real line (subharmonic bifurcation);

(c) two pairs of conjugate eigenvalues collide at two conjugate points on the unit circle and leave it (Krein crunch or oscillatory bifurcation).

It must be remembered that a bifurcation involving two eigenvalues with the same sign of the Krein signature $\kappa(\theta) = \mathrm{sign}(\mathrm{i}(\dot{\xi} \cdot \xi^* - \dot{\xi}^* \cdot \xi))$ is not possible [1].

The basic features of the Floquet multipliers at the anti-continuous limit for bright and dark breathers are the following.

- For bright breathers, there are $N-1$ Floquet multipliers corresponding to the oscillators at rest. They are degenerate at $\theta = \pm 2\pi\omega_0/\omega_b)$. The eigenvalues at $0 < \theta < \pi$ have $\kappa > 0$ while the ones at $-\pi < \theta < 0$ have $\kappa < 0$. If $\theta = 0$ or π, $\kappa = 0$. In addition, there are two eigenvalues at $1 + 0\mathrm{i}$, corresponding to the excited oscillator.
- For dark breathers, there are two eigenvalues at $\theta = \pm 2\pi\omega_0/\omega_b$ corresponding to the oscillator at rest, and there are $2(N-1)$ eigenvalues at $1 + 0\mathrm{i}$ corresponding to the excited oscillators.

When the coupling is switched on, the evolution of the Floquet multipliers for bright breathers is rather different from the case of dark breathers:

- For a bright breather, the Floquet eigenvalues corresponding to the oscillators at rest lose their degeneracy and expand on two bands of eigenvalues, called the phonon bands. Their corresponding eigenmodes are extended. These two bands move on the unit circle and eventually cross each other. In this case, eigenvalues of different Krein signature can collide and abandon the unit circle through subharmonic or oscillatory bifurcations. In addition, some eigenvalues can abandon the bands and become localized [23]. A pair of complex conjugate eigenvalues can collide at $1 + 0\mathrm{i}$ leading to a harmonic bifurcation or collide with the phonon band through a oscillatory bifurcation.
- For a dark breather, the eigenvalues corresponding to the excited oscillators, with extended phonon eigenmodes, can either depart from the unit circle along the real axis (harmonic bifurcation) or move along the unit circle. In the last case, they can collide with the eigenvalue corresponding to the rest oscillator (with localized eigenmode) through a Krein crunch. Eventually, if the on-site potential is non-symmetric, the eigenvalues collide at $-1 + 0\mathrm{i}$, leading to a cascade of subharmonic bifurcations.

The study of breather stability can be complemented by means of Aubry's band theory [1]. It consists in studying the linearized system (8) for $E \neq 0$, with the corresponding family of Floquet operators $\mathcal{F}_E$. For each operator $\mathcal{F}_E$ there are $2 \times N$ Floquet multipliers. A Floquet multiplier can be written as $\lambda = \exp(\mathrm{i}\theta)$. θ is called the Floquet argument. If θ is real then $|\exp(\mathrm{i}\theta)| = 1$ and the corresponding eigenfunction of (8) is bounded and corresponds to a stability mode; if θ is complex, it corresponds to an instability mode. The set of points (θ, E), with θ real, has a band structure. The breather is stable if there are $2 \times N$ band intersections (including tangent points with their multiplicity) with the axis $E = 0$. The bands are reduced to the first Brillouin zone $(-\pi, \pi]$ and are symmetric with respect to the axis $\theta = 0$. The fact that $\mathcal{F}_0$ has always a double $+1$ eigenvalue corresponding to the phase mode $\dot{u}(t)$ manifests as a band which is tangent to the $E = 0$ axis.

For the uncoupled system, the structure of the stable and unstable bands is completely explained by the theory (although it has to be calculated numerically). For the coupled system, such structure is expected to change in a continuous way in terms of the parameter ε. We will use band theory to predict the evolution of the eigenvalues of $\mathcal{F}_0$ when a model parameter is changed.

At zero coupling, the bands corresponding to the oscillators at rest can be analytically calculated from the equation

$$\ddot{\xi}_n + \omega_0^2 \xi_n = E\xi_n; \tag{11}$$

they are given by $E = \omega_0^2 - \omega_b^2\theta^2/(2\pi)^2$. The bands corresponding to the $N-1$ excited oscillators are a deformation of the band corresponding to the oscillator at rest (which will be called *rest*

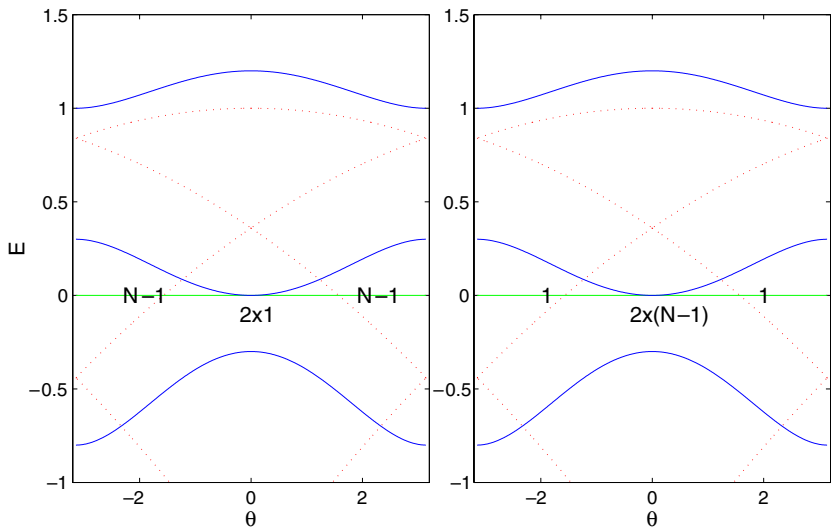

Figure 2. Band scheme for bright (left) and dark (right) breathers with soft potential. The continuous lines correspond to the excited oscillators and are numbered downwards starting from zero. The dotted curves correspond to the oscillator at rest.

bands) and one of them must be tangent to $E = 0$ axis at $(\theta, E) = (0, 0)$ [1]. The bands are bounded from above and numbered starting from the top, the zeroth band being the first one. If the on-site potential is soft the first band will be tangent to the $E = 0$ axis at $(0, 0)$ with positive curvature. If the on-site potential is hard, the tangent band at $(0, 0)$ will be the second one, and will have negative curvature [21]. At the anticontinuous limit the band scheme of a bright and a dark breather are similar, differing only in the number of bands that corresponds to the oscillators at rest or to the excited oscillators (*excited bands*) as shown in figures 2 and 3.

The bright breather has only one band tangent to the axis $E = 0$ and that band cannot leave this position because, when the coupling is switched on, there must be a tangent band corresponding to the phase mode. The situation is totally different for a dark breather: there are $N - 1$ bands tangent to the $E = 0$ axis and $N - 2$ of them can move without any restriction. If some of them move upwards, the intersection points disappear, which implies that some Floquet arguments become complex or, equivalently, that some Floquet multipliers abandon the unit circle and the breather becomes unstable.

5. Dark breathers with soft on-site potentials

Let us consider a model with a cubic on-site potential given by

$$V(u_n) = \tfrac{1}{2}\omega_0^2 u_n^2 - \tfrac{1}{3}u_n^3, \tag{12}$$

that is, $\phi'(u_n) = -u_n^2$ in the dynamical equations (4). Figure 4 represents the Floquet multipliers for $\varepsilon \neq 0$. The left side of the figure shows the Floquet multipliers of a stable bright breather for a coupling $\varepsilon = 0.1$. However, as can be seen on the right side of the figure, the dark breather experiences a multiple harmonic bifurcation as soon as the coupling is switched on. Therefore, for a lattice with a cubic on-site potential and attractive interaction, dark breathers exist but they are unstable for every value of the coupling.

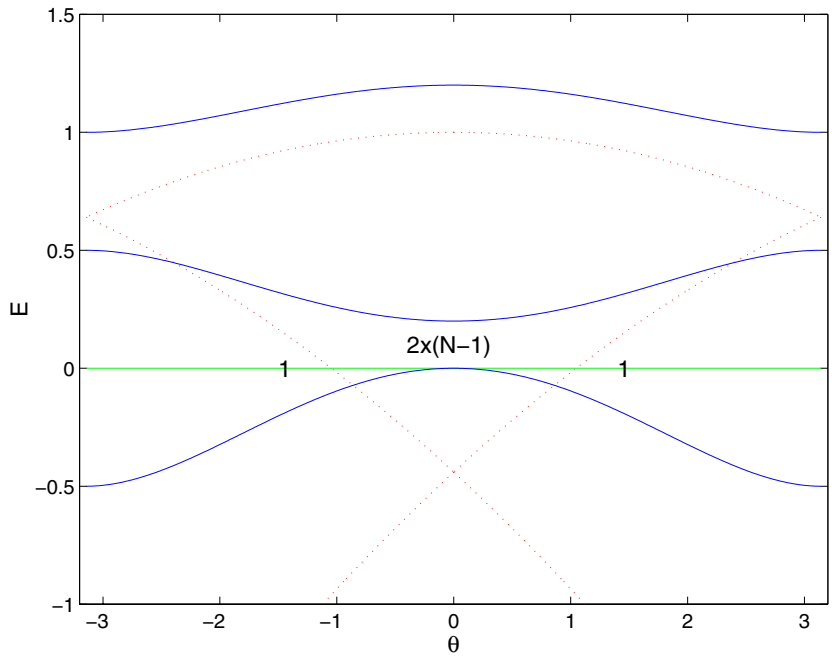

Figure 3. Band scheme for a dark breather with hard potential at zero coupling. The continuous curves correspond to the excited oscillators and are numbered downwards starting from zero. The dotted curves correspond to the oscillator at rest.

This problem can be investigated by means of Aubry's band analysis. It has given us an explanation for the previous behaviour and also a guide for modifying the model in order to obtain stable dark breathers. The bands at zero coupling can be seen in figure 5.

As explained above and shown in figure 4, the cubic dark breather becomes unstable for any attractive coupling $\varepsilon > 0$ through harmonic bifurcations. This is easily understood in terms of the band structure: $N-2$ tangent bands move upwards, which is mathematically demonstrated in [24]. They lose the tangent points with the $E = 0$ axis as figure 6 shows. Therefore, in order that the breather can be stable all the excited bands except one have to move downwards, transforming the points tangent to the $E = 0$ axis into intersection points. A straightforward alternative is to change the sign of the parameter ε in (1). This is equivalent to using a dipole–dipole coupling potential $W(u) = \sum_n u_{n+1}u_n$, i.e., the Hamiltonian can be written as

$$H = \sum_n \left(\tfrac{1}{2}\dot{u}_n^2 + \tfrac{1}{2}\omega_0^2 u_n^2 - \tfrac{1}{3}u_n^3 + \tfrac{1}{2}\varepsilon(u_{n+1}u_n)\right) \tag{13}$$

with $\varepsilon > 0$. This repulsive interaction has been used recently for DNA-related models [25]–[30]. The dynamical equations with repulsive interaction and cubic on-site potential become

$$\ddot{u}_n + \omega_0^2 u_n - u_n^2 + \varepsilon(u_{n-1} + u_{n+1}) = 0, \tag{14}$$

and the linear stability equations become

$$\ddot{\xi}_n + \omega_0^2 \xi_n - 2u_n\xi_n + \varepsilon(\xi_{n-1} + \xi_{n+1}) = 0. \tag{15}$$

Figure 7 displays the band structure at $\varepsilon = 0.015$ for this system. The $N-2$ bands that are allowed to move will perform a downwards movement and therefore the breather is stable.

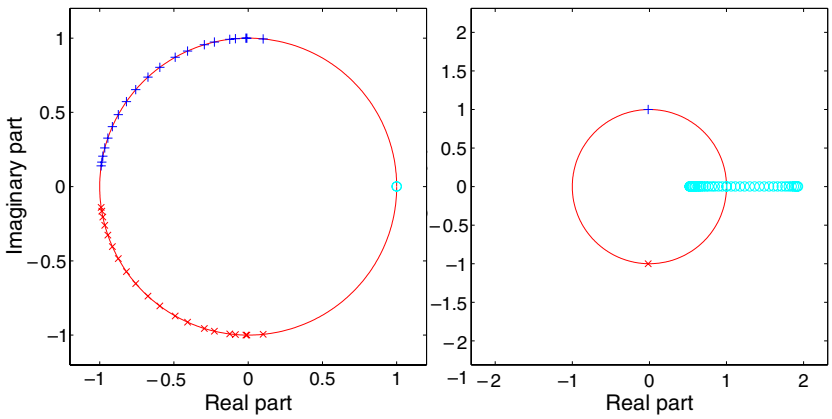

Figure 4. Evolution of the Floquet multipliers with cubic on-site potential and attractive interaction when the coupling is switched on for (left) the bright breather at $\varepsilon = 0.1$, which is linearly stable, although reaching a possible bifurcation at -1; (right) the dark breather at a much smaller coupling parameter $\varepsilon = 0.004$. The breather frequency is $\omega_b = 0.8$.

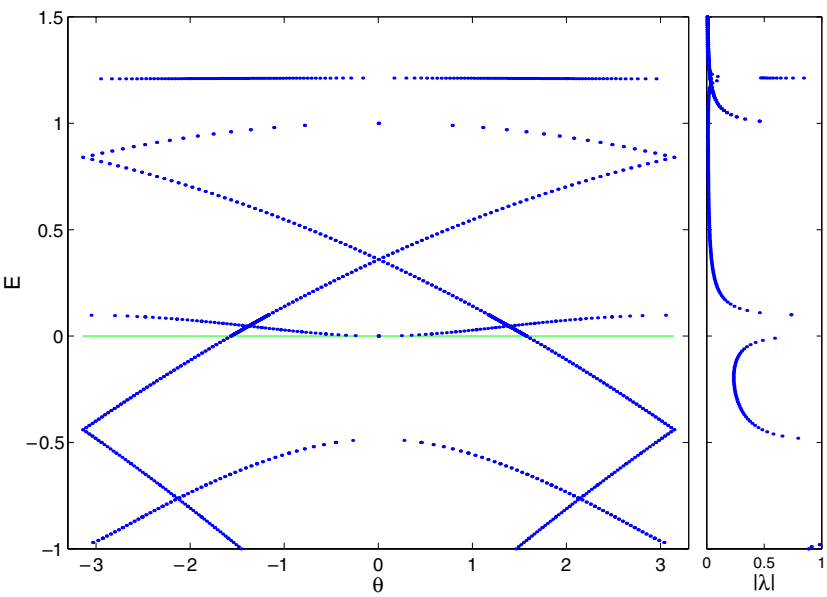

Figure 5. Band structure at zero coupling for a cubic on-site potential. The right part of the figure plots the moduli of the unstable Floquet multipliers that are smaller than 1, their inverses being the unstable multipliers. Frequency $\omega_b = 0.8$.

A further increase of ε leads to Krein crunches. They are caused by the mixing of the rest bands and the excited bands, that produces 'wiggles' in the excited bands and gaps appear between them [31]. When these bands move downwards and the 'wiggles' cross the $E = 0$ axis, intersection points are lost but recovered when the coupling increases. This manifests as the appearance of 'instability bubbles'. These instabilities depend on the size of the system, as

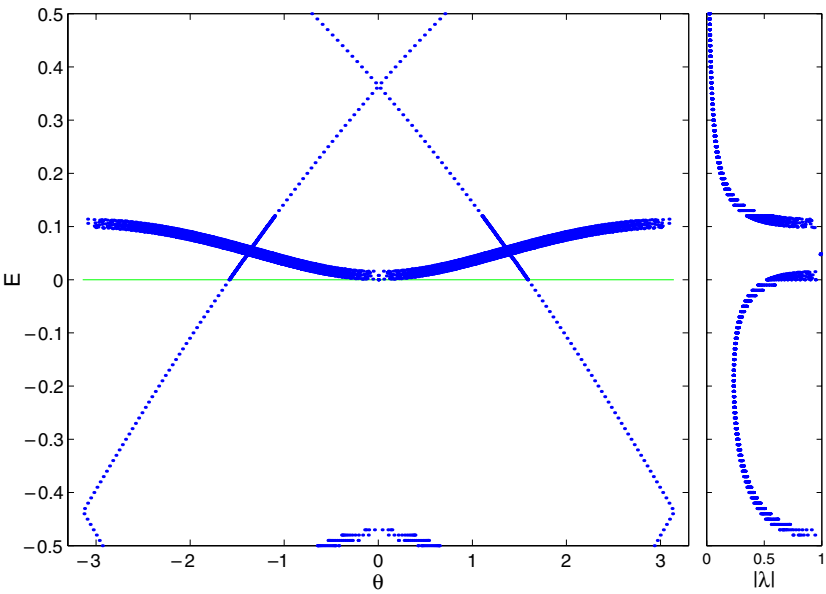

Figure 6. Band structure of a dark breather with cubic on-site potential and attractive interaction at very low coupling ($\varepsilon = 0.004$). Frequency $\omega_b = 0.8$.

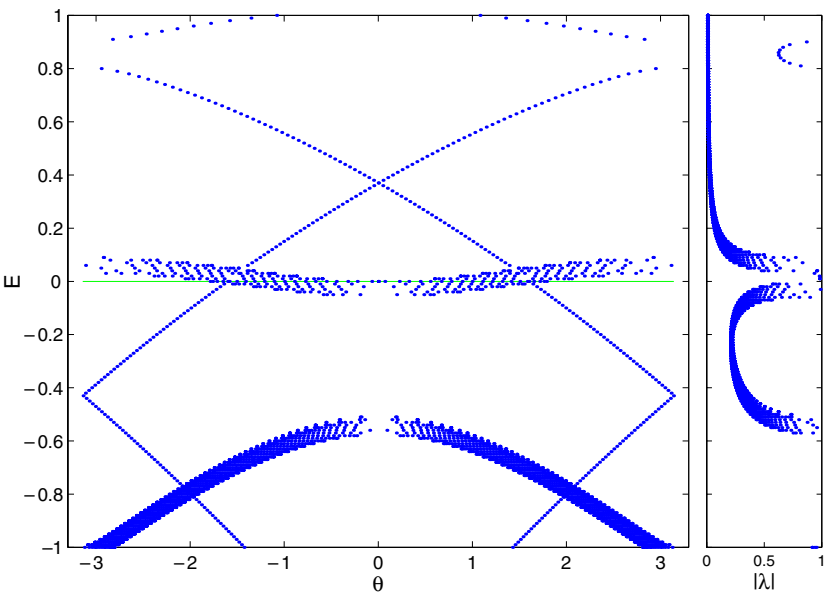

Figure 7. Band structure of a dark breather with cubic on-site potential and repulsive interaction at $\varepsilon = 0.015$. Frequency $\omega_b = 0.8$.

will be shown in section 7. The system will eventually become unstable through a cascade of subharmonic bifurcations when the lower excited band goes below the $E = 0$ axis, losing the intersection points at $\theta = \pm\pi$ (see figure 8).

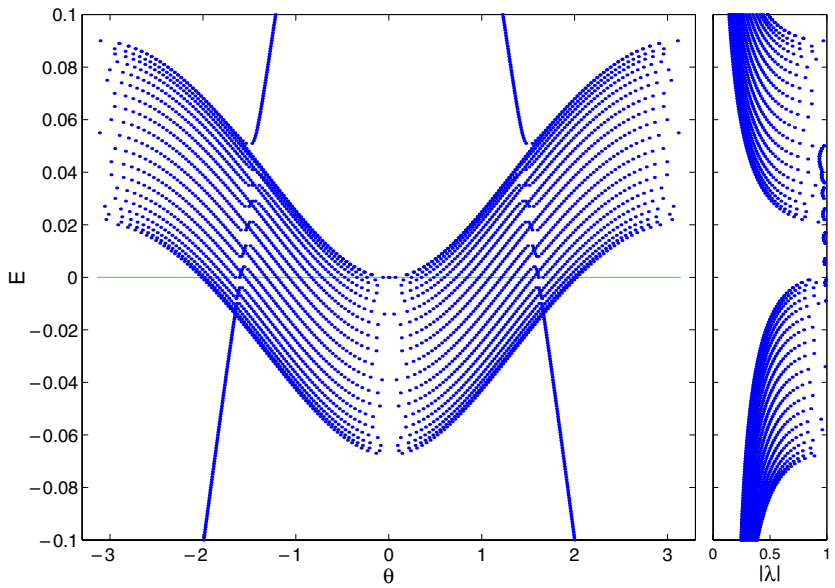

Figure 8. Band structure of a dark breather with cubic on-site potential and repulsive interaction at $\varepsilon = 0.017$ and $\omega_b = 0.8$. Note the 'wiggles' that appear when the excited bands and the rest band mix. A further increase of the coupling parameter ε will make the excited bands fall below $E = 0$ producing subharmonic bifurcations.

We have obtained dark breathers for systems with cubic on-site potential and attractive or repulsive interaction even though dark breathers with attractive coupling are not stable. Figure 9 shows two different examples of dark breathers for these two types of coupling. Notice that the oscillator with small amplitude is in phase with its neighbours when the system is unstable (left) while it is in anti-phase when it is stable (right).

This type of behaviour is general for other soft on-site potentials as it can be obtained using, for example, the Morse potential given by

$$V(u_n) = D(\exp(-bu_n) - 1)^2. \tag{16}$$

For this system, dark breathers maintain their stability until the coupling parameter reaches the value $\varepsilon = 0.024$. From this value Krein bifurcations appear. These bifurcations are harmless in the sense that they preserve the dark localization, but the breather becomes quasiperiodic with a frequency superimposed on the breather one. For $\varepsilon > 0.033$, the system becomes unstable due to subharmonic bifurcations. Figure 10 shows this behaviour in terms of the corresponding Floquet multipliers for two different values of the coupling. With this potential, it has been described [11] that for values of the ω_b close to the linear frequency ω_0 (in fact, slightly above it), oscillatory instabilities can bring about the movement of dark breathers, when the corresponding eigenvalue is asymmetric and localized. This does not happen for frequencies far enough from ω_0 such as the ones of the order we present here.

An interesting variation of this scheme occurs if we consider symmetric on-site potentials such as the quartic soft potential given by

$$V(u_n) = \tfrac{1}{2}\omega_0^2 u_n^2 - \tfrac{1}{4}u_n^4. \tag{17}$$

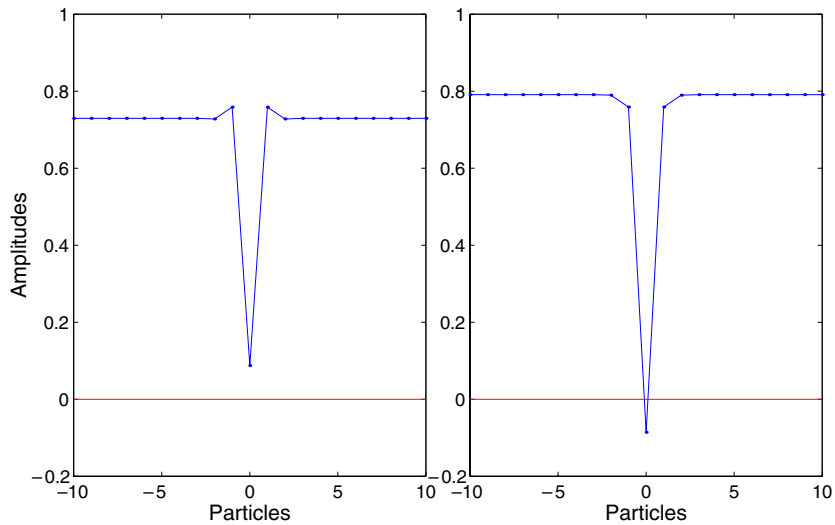

Figure 9. Dark breather profile for a cubic potential with attractive interaction (left) and with repulsive interaction(right), at $\varepsilon = 0.023$. The last one is stable.

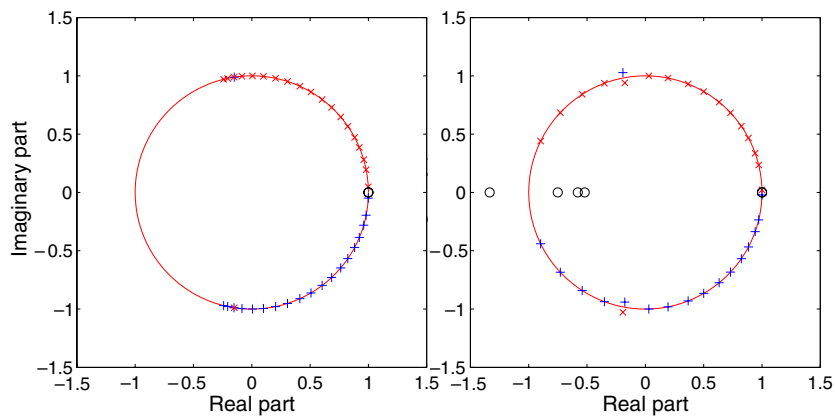

Figure 10. Evolution of the Floquet eigenvalues for a Morse on-site potential and repulsive coupling. Left: $\varepsilon = 0.024$; the system is still stable. Right: $\varepsilon = 0.035$; the system becomes unstable due to subharmonic bifurcation and Krein crunches.

In this case the potential is symmetric and no subharmonic bifurcations at $\lambda = \pm 1$ occur because the bands are gapless at $\theta = \pm\pi$. This characteristic enlarges the stability range (see figure 11). The system eventually becomes unstable (apart from the reentrant instabilities due to Krein crunches) through harmonic bifurcations.

6. Dark breathers with hard on-site potentials

The band scheme of a system with hard on-site potential at $\varepsilon = 0$ is shown in figure 3. There are $N - 1$ bands tangent to the axis $E = 0$. It is clear that the breather will remain stable provided that the tangent bands keep the intersection points when the degeneracy is raised with $\varepsilon \neq 0$. In this system it means that the $N - 2$ bands that can move will perform an upwards movement.

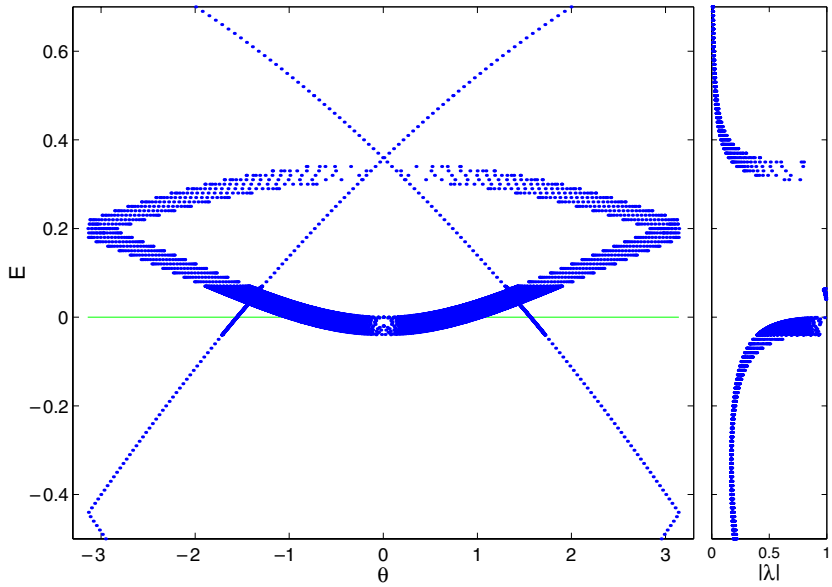

Figure 11. Band structure for a dark breather with quartic soft on-site potential and repulsive coupling. Note the absence of gaps at $\theta = \pm\pi$ which enlarges the stability range. Parameters: $\varepsilon = 0.018$ and $\omega_b = 1.2$.

Therefore, the dark breather will be stable with an attractive coupling potential. We have used for the numerics the quartic hard on-site potential, that is

$$V(u_n) = \tfrac{1}{2}\omega_0^2 u_n^2 + \tfrac{1}{4}u_n^4. \tag{18}$$

The Hamiltonian is then

$$H = \sum_n (\tfrac{1}{2}\dot{u}_n^2 + \tfrac{1}{2}\omega_0^2 u_n^2 + \tfrac{1}{3}u_n^3 + \tfrac{1}{2}\varepsilon(u_{n+1} - u_n)^2). \tag{19}$$

Figure 12 shows that at $\varepsilon = 0.01$ the tangent bands have moved upwards and, therefore, the stability of the system is maintained. The system loses its stability at $\varepsilon = 0.022$ where a harmonic bifurcation appears. In figures 13 and 14 (left) the band structure and the corresponding Floquet multipliers at $\varepsilon = 0.041$ are represented. The instability mode, shown in figure 14 with its multipliers, is an asymmetric extended one. Simulations performed perturbing with it the dark breather give rise to an small oscillation with both sides of the chain out of phase, superimposed on the dark breather one, but the *darkness* is preserved. After that, there are Krein crunches due to the band mixing with the usual properties.

7. Finite size effects

This final section is dedicated to commenting on some preliminary results relative to the finite size effects on instability of dark breathers. Important differences appear with respect to the case of bright breathers [31].

In the case of bright breathers, there are two kinds of size-dependent bifurcation. The origin of these relies on the nature of the localization of the colliding eigenvalues. If the colliding eigenvalues are extended, there appear 'instability bubbles', i.e. the Floquet eigenvalues abandon

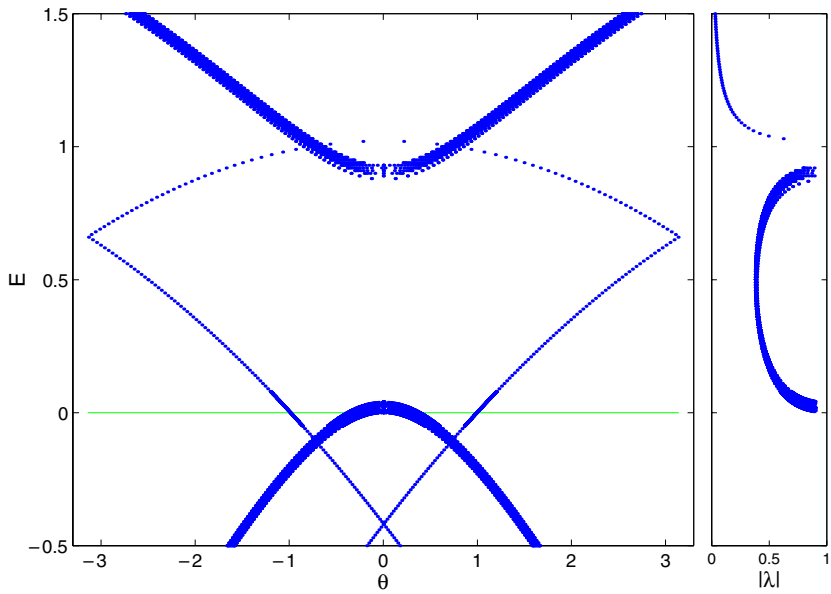

Figure 12. Band structure for a quartic hard on-site potential with attractive interaction at $\varepsilon = 0.01$ and $\omega_b = 1.2$.

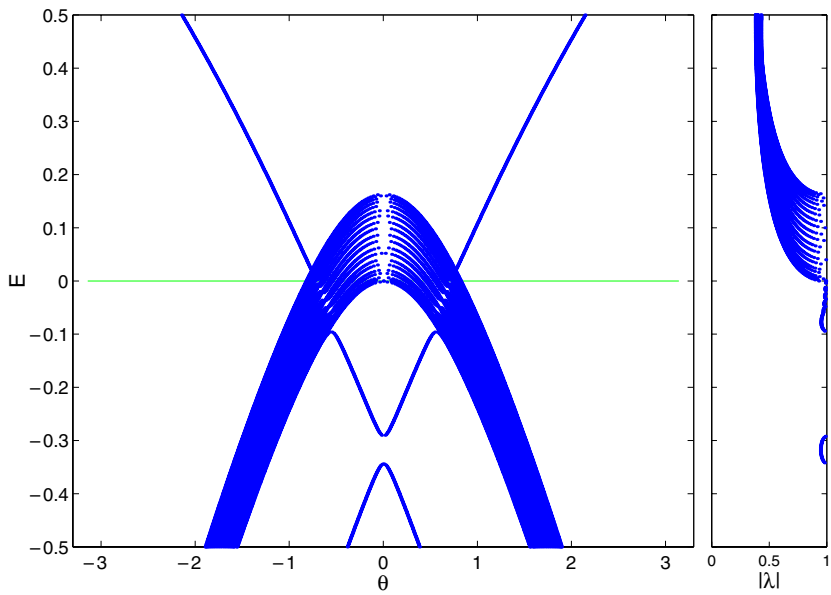

Figure 13. Zoom of the band structure for a quartic hard on-site potential with attractive interaction at $\varepsilon = 0.041$ and $\omega_b = 1.2$.

the unit circle after the collision but return afterwards. These bifurcations disappear when the system is infinite. Alternatively, a localized eigenvalue can collide with a band of extended eigenvalues. In this case, the instability bubbles also occur but they persist even though the system is infinite.

In order to study the case of dark breathers, we have chosen a Morse on-site potential with repulsive interaction. As a result of this analysis, the collision of extended eigenvalues always

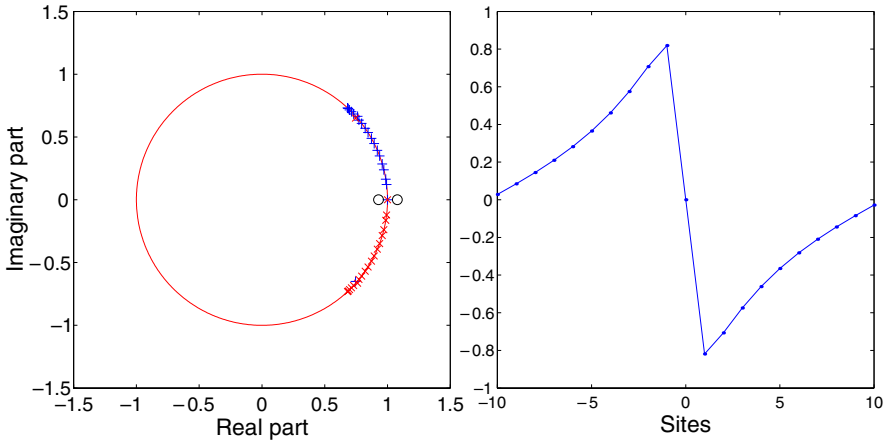

Figure 14. Left: Floquet multipliers with a quartic hard on-site potential and attractive interaction at $\varepsilon = 0.041$ and $\omega_b = 1.2$. A harmonic and a small Krein instability appear. Right: the velocity components (the position ones are zero) of the eigenvalue corresponding to the harmonic instability.

implies a cascade of subharmonic bifurcations (see section 4) independently of the size of the system. This is because they are due to excited bands, whose Floquet arguments belong to the first Brillouin zone, losing intersections at $\theta = \pi$. This is different from the case of bright breathers where this kind of instability is due to modes corresponding to oscillators at rest and the bands must be reduced to the first Brillouin zone.

Also, an eigenvalue corresponding to an extended mode can collide with a localized mode. In this case, the rest (localized mode) band and the excited (extended modes) bands mix (see figure 15). There appear 'wiggles' that imply the opening of gaps in the band scheme, which are the origin of the instability bubbles. However, when the size of the system is increased, the wiggles widen until they occupy almost the width of the quasi-continuous extended mode bands. This fact implies that, although the instability bubbles disappear, the Krein crunches are unavoidable (see figure 16). Nevertheless, the breathers are robust despite the existence of these instabilities.

8. Dark breather stability in dissipative systems

There appear some important differences in the study of the stability of dark breathers in dissipative systems with respect to the Hamiltonian case.

In order to perform this study, we start from the dissipative Frenkel–Kontorova model [32]:

$$\ddot{u}_n + \gamma \dot{u}_n + V'(u_n) + \varepsilon(2u_n - u_{n+1} - u_{n-1}) = F \sin \omega_b t \tag{20}$$

where γ is a damping parameter and F the amplitude of an external force.

In the anticontinuous limit, there are no bands tangent to the $E = 0$-axis (figure 17(a)). This implies that, when the coupling is introduced, there is no loss of intersections of the bands with independence of the sign of the coupling constant (ε). Furthermore, the bands corresponding to the oscillator at rest do not mix with the band of the background and oscillatory instabilities do not appear. These phenomena are shown in figure 17.

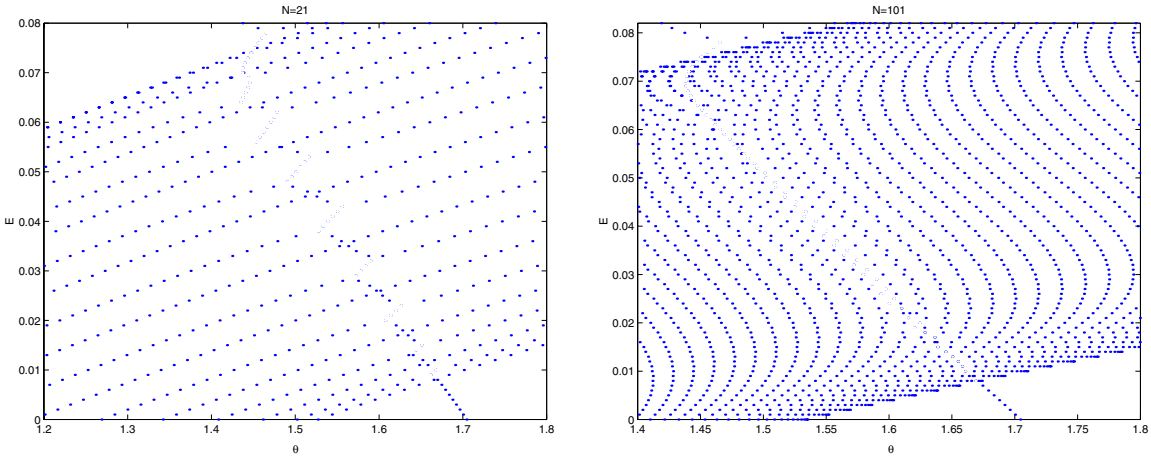

Figure 15. Zoom of the band scheme for $N = 21$ and 101 and a Morse potential ($\varepsilon = 0.02$ and $\omega_b = 0.8$). The appearance of wiggles can be observed when $N = 21$, which are much wider when $N = 101$; these wiggles are almost invisible because they occupy the width of the band.

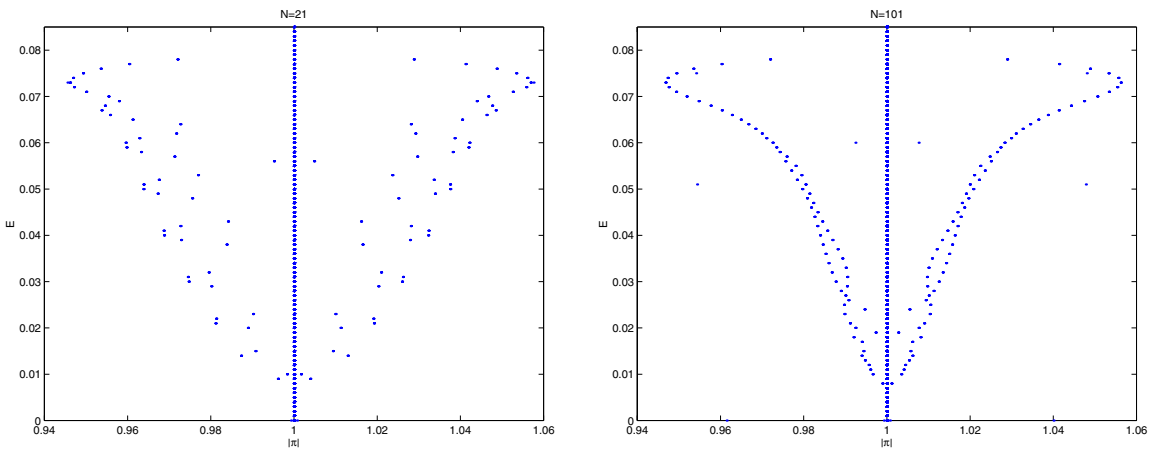

Figure 16. Moduli of the Floquet eigenvalues corresponding to the Krein crunches for $N = 21$ and 101 and a Morse potential ($\varepsilon = 0.02$ and $\omega_b = 0.8$). The appearance of instability bubbles can be observed when $N = 21$. However, these bubbles transform into an instability that persists up to a value of the coupling for which the breather is unstable because of the subharmonic bifurcations.

9. Conclusions

In this paper we have explored the existence and stability of dark breathers in one-dimensional Klein–Gordon models, for frequencies far enough from the linear frequencies for the DNLS approximation be justified . We have found stable dark breathers in several types of them. For systems with soft on-site potential, there are no stable dark breathers if the coupling between particles is attractive, but with a repulsive coupling the stability is assured for fairly high values

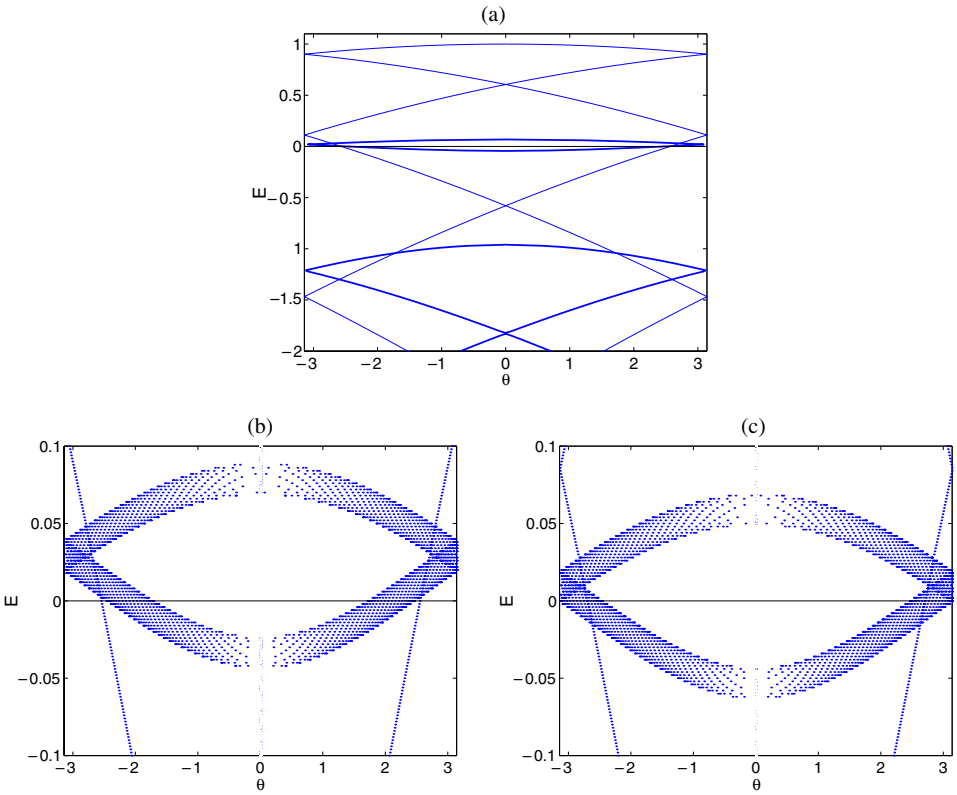

Figure 17. Band diagrams in the anticontinuous limit (top) and for a coupling $\varepsilon = \pm 0.005$ (bottom) for a dark breather in the Frenkel–Kontorova model. The parameters are $\omega_b = 0.2\pi$, $\gamma = 0.02$ and $F = 0.02$. (b) An attractive interaction potential; (c) a repulsive potential. The dark breather is stable in both cases.

of the coupling parameter ε. As ε increases, instability bifurcations due to Krein crunches take place as a consequence of the band mixing between the rest oscillator band and the dark background. Eventually, the system experiences subharmonic bifurcations at -1 that make the breather unstable. If the soft on-site potential is symmetric the subharmonic bifurcations are avoided and the final instability is caused by harmonic bifurcations. For systems with hard on-site potentials, the situation is reversed and the dark breathers are stable with attractive coupling and unstable with repulsive coupling. They experience harmonic bifurcations at $+1$ apart from the Krein crunches. An analysis of larger systems shows that these bifurcations persist even though the system is infinite. Dissipative systems are, however, stable for both types of coupling.

We are now engaged on the project of performing a wider study of dark breathers in dissipative systems. Another interesting aspect is to study the relationship of the vibration pattern of dark breathers with the hardness of the on-site potential and the type of coupling. The ansatz $u_n \to (-1)^n u_n$, which transforms repulsive coupling into attractive and vice versa for symmetric potentials, suggests, and it has been shown for the DNLS equations, and we also have checked numerically, that the stability conditions are reversed are low coupling, but the bifurcations for $|\omega_b - \omega_0|$ large enough, highly asymmetric potentials as found in chemical and biological systems and larger coupling are worth studying.

Acknowledgments

This work has been supported by the European Union under the RTN project, LOCNET, HPRN-CT-1999-00163. JFRA acknowledges Informatics and Mathematical Modelling at DTU for hospitality while this work was started and Yu B Gaididei for valuable suggestions. JC acknowledges an FPDI grant from La Junta de Andalucía.

References

[1] Aubry S 1997 Breathers in nonlinear lattices: existence, linear stability and quantization *Physica* D **103** 201–50
[2] Flach S and Willis C R 1998 Discrete breathers *Phys. Rep.* **295** 181–264
[3] MacKay R S and Aubry S 1994 Proof of existence of breathers for time-reversible or Hamiltonian networks of weakly coupled oscillators *Nonlinearity* **7** 1623–43
[4] Marín J L and Aubry S 1995 Breathers in nonlinear lattices: numerical methods based on the anti-integrability concept *Nonlinear Klein–Gordon and Schrödinger Systems: Theory and Applications* ed L Vázquez, L Streit and VM Pérez-García (Singapore: World Scientific) pp 317–23
[5] Zakharov V E and Shabat A B 1972 Exact theory of two-dimensional self-focusing and one-dimensional self-modulation of waves in nonlinear media *Sov. Phys.–JETP* **34** 62–9
[6] Zakharov V E and Shabat A B 1973 Interaction between solitons in a stable medium *Sov. Phys.–JETP* **37** 823
[7] Kivshar Yu S and Peyrard M 1992 Modulational instabilities in discrete lattices *Phys. Rev.* A **46** 3198
[8] Kivshar Yu S, Królikowski W and Chubykalo O A 1994 Dark solitons in discrete lattices *Phys. Rev.* E **50** 5020–32
[9] Konotop V V and Takeno S 1999 Stationary dark localized modes: discrete nonlinear Schrödinger equations *Phys. Rev.* E **60** 1001–8
[10] Johansson M and Kivshar Yu S 1999 Discreteness-induced oscillatory instabilities of dark solitons *Phys. Rev. Lett.* **82** 85
[11] Morgante A M, Johansson M, Kopidakis G and Aubry S 2002 Standing waves instabilities in a chain of nonlinear coupled oscillators *Physica* D **162** 53
[12] Denardo B, Gakvin B, Greenfield A, Larraza A and Puttermann S 1992 Observations of localized structures in nonlinear lattices: domain walls and kinks *Phys. Rev. Lett.* **68** 1730
[13] Dusi R and Wagner M 1995 Gauss procedure for the construction of self-localized solitons in discrete systems *Phys. Rev.* B **51** 15847–55
[14] Daumont I, Dauxois T and Peyrard M 1997 Modulational instability: first step towards energy localization in nonlinear lattices *Nonlinearity* **10** 617–30
[15] Peyrard M and Bishop A R 1989 Statistical-mechanics of a nonlinear model for DNA denaturation *Phys. Rev. Lett.* **62** 2755–8
[16] Flach S 1995 Existence of localized excitations in nonlinear Hamiltonian lattices *Phys. Rev.* E **51** 1503–7
[17] Flach S 1995 Obtaining breathers in nonlinear Hamiltonian lattices *Phys. Rev.* E **51** 3579–87
[18] Marín J L and Aubry S 1996 Breathers in nonlinear lattices: numerical calculation from the anticontinuous limit *Nonlinearity* **9** 1501–28
[19] Marín J L, Aubry S and Floría L M 1998 Intrinsic localized modes: discrete breathers. Existence and linear stability *Physica* D **113** 283–92
[20] MacKay R S and Sepulchre J A 1998 Stability of discrete breathers *Physica* D **119** 148–62
[21] Marín J L 1997 Intrinsic localised modes in nonlinear lattices *PhD Dissertation* University of Zaragoza, Department of Condensed Matter
[22] Sanz-Serna J M and Calvo M P 1994 *Numerical Hamiltonian Problems* (London: Chapman and Hall)
[23] Baesens C, Kim S and MacKay R S 1998 Localised modes on localised equilibria *Physica* D **113** 242–7
[24] Archilla J F R, Cuevas J, Sánchez-Rey B and Alvarez A 2002 Demonstration of the stability or instability of multibreathers at low coupling *Physica* D submitted (*Preprint* nlin.PS/0208014)

[25] Christiansen P L, Gaididei Yu B, Johansson M, Rasmussen K Ø, Mezentsev V K and Rasmussen J J 1998 Solitary excitations in discrete two-dimensional nonlinear Schrödinger models with dispersive dipole–dipole interactions *Phys. Rev.* B **57** 11303–18

[26] Gaididei Y B, Mingaleev S F and Christiansen P L 2000 Curvature-induced symmetry breaking in nolinear Schrödinger models *Phys. Rev.* E **62** R53–6

[27] Archilla J F R, Christiansen P L and Gaididei Yu B 2001 Interplay of nonlinearity and geometry in a DNA-related, Klein–Gordon model with long-range dipole–dipole interaction *Phys. Rev.* E **65** 016609–16

[28] Christiansen P L, Gaididei Yu B and Mingaleev S F 2001 Effects of finite curvature on soliton dynamics in a chain of nonlinear oscillators *J. Phys.: Condens. Matter* **13** 1181–92

[29] Cuevas J, Archilla J F R, Gaididei Yu B and Romero F R 2002 Static and moving breathers in a DNA model with competing short- and long-range dispersive interactions *Physica* D **163** 106–26

[30] Cuevas J, Palmero F, Archilla J F R and Romero F R 2002 Moving breathers in a bent DNA-related model *Phys. Lett.* A **299** 221–5

[31] Marín J L and Aubry S 1998 Finite size effects on instabilities of discrete breathers *Physica* D **119** 163–74

[32] Marín J L, Falo F, Martínez P J and Floría L M 2001 Discrete breathers in dissipative lattices. *Phys. Rev.* E **63** 066603